An Addressable Microfluidics device for Nondestructive Manipulation of Cells and Chemicals within Live Cultures

Anh Tong,[1] Quang Long Pham,[1] Vatsal Shah,[2,3] Akshay Naik,[4] Paul Abatemarco,[1] and Roman Voronov[1,†]

[1]Otto H. York Department of Chemical and Materials Engineering, New Jersey Institute of Technology, Newark, NJ, USA
[2]Ying Wu College of Computing Sciences, Department of Computer Science, New Jersey Institute of Technology, Newark, NJ 07102, USA
[3]Federated Department of Mechanical and Industrial Engineering, New Jersey Institute of Technology, Newark, NJ 07102, USA
[4]Helen and John C. Hartmann Department of Electrical and Computer Engineering, New Jersey Institute of Technology, Newark, NJ 07102, USA

[†]Address correspondence to Prof. Roman S. Voronov, Otto H. York Department of Chemical and Materials Engineering, New Jersey Institute of Technology, Newark, NJ 07102, USA. Electronic mail: *rvoronov@njit.edu*, Fax: +1 973 596 8436, Tel: +1 973 642 4762

ABSTRACT

According to the U.S. Department of Health & Human Services, nearly 115,000 people in the U.S needed a lifesaving organ transplant in 2018, while only ~10% of them have received it. Yet, almost no artificial FDA-approved products[1] are commercially available today – three decades after the inception of tissue engineering. It is hypothesized that the major bottlenecks restricting its progress stem from lack of access to the inner pore space of the scaffolds. Specifically, the inability to deliver nutrients to, and clear waste from, the center of the scaffolds limits the size of the products that can be cultured. Likewise, the inability to monitor, and control, the cells after seeding them into the scaffold results in nonviable tissue, with an unacceptable product variability. To resolve these bottlenecks, we present a prototype addressable microfluidics device capable of non-invasive fluid and cell manipulation (i.e., both additive and subtractive manufacturing) within living cell cultures. As proof-of-concept, we demonstrate its ability to perform additive manufacturing by seeding cells in patterns (including co-culturing multiple cell types); and subtractive manufacturing, by removing surface adherent cells via targeted trypsin release. Additionally, we show that the device is capable of sampling fluids non-invasively, from any location within the cell culturing chamber. Finally, the on-chip plumbing is completely automated using external electronics. This opens up the possibility to perform long-term computer-driven tissue engineering experiments, where the cell behavior is modulated in response to the non-invasive observations throughout the whole duration of the cultures. It is expected that the proof-of-concept technology will eventually be scaled up to 3D addressable microfluidic scaffolds, capable of overcoming the limitations bottlenecking the transition of tissue engineering technologies to the clinical setting.

I. INTRODUCTION

According to the U.S. Department of Health & Human Services, nearly 115,000 people in the U.S needed a lifesaving organ transplant in 2018, while only ~10% of them have received it. Yet, almost no FDA-approved[2] artificial organs are commercially available today – three decades after the inception[3] of tissue engineering and after billions of dollars invested into its development. Therefore, a new approach to biomanufacturing is needed. However, there are major obstacles restricting the progress of complex organ and tissue recreation *in vitro*:

1) Product Size Limitations – due to the lack of an active vasculature and blood circulation within lab-grown tissues, it is difficult to deliver nutrients to / clear metabolic waste from the inner pore space of large (organ-sized) scaffolds. As a result, cell survival in the deep portions of the large scaffolds is compromised due to hypoxia and insufficient nutrient availability. Specifically, scaffolds with dimensions larger than 3.8x3.8x3.8mm^3 are classified as *large-volume*, and constructs larger than that (e.g., 5.6x5.6x5.6 mm) have been found to result in areas of hypoxia after 3 days of culture.[4, 5] Consequently, out of the three FDA-approved cellular therapies, one (LAVIV injectable fibroblasts for wrinkle treatment) is a suspension of disconnected cells and two (MACI knee cartilage implant and GINTUIT topical treatment of dental wounds) are flat strips of tissue.[2] No artificial 3D solid organs or complex tissues are currently available.

2) Sacrificial Analysis – due to the inability to sample cells and fluids from within scaffolds nondestructively and because live, long-term 3D microscopy is challenging. This makes it necessary to perform destructive chemical assays at the conclusion of each experiment, by crushing the cultured scaffold. As a result, a different sample has to be cultured for each new time point. This balloons the cost of experiments and slows down the scientific progress tremendously.

3) Product Variability – due to the absence of a native central nervous system and lack of access to the cells post seeding, there is no orchestration over their actions within the scaffolds. For example, even if one were to bioprint (i.e., deposit the cells into precise locations within a scaffold) the perfect artificial tissue, the cells within it would be free to do a number of undesirable things afterwards: a) migrate away uncontrollably,[6] b) differentiate into the wrong tissue type (e.g., a patient grew mucus tissue in her spine, as a result of stem cell therapy),[7] and c) deposit tissue in the wrong locations and occlude the scaffold pores. All this leads to nonviable tissue and poor product consistency. In fact, a survey of 16 big pharmaceutical companies found that "product consistency is possibly the single greatest challenge facing the field" of regenerative medicine.[8]

4) Technology Adoption Barriers – Even if one could generate the perfect tissue in a laboratory, training hospital staff in custom culturing protocols for each new product remains another critical hurdle holding back biomanufacturing technologies from entering the market.

In this study, we hypothesize that in order to overcome these obstacles, an ideal scaffold should be composed of the following elements: (1) Active "Vasculature" for distributing metabolites and clearing waste throughout *organ-sized* scaffolds; (2) Nondestructive Sampling of the cells and of the fluids within them for *ex-situ* chemical analysis; (3) Tissue Modulation via cell and bio-active chemical (e.g., chemo-attractants, growth and differentiation factors, drugs, etc.) delivery; (4) Long-term Live Microscopy observation of the cell behavior and tissue growth, and (5) Automated Spatiotemporal Control over the tissue development in a closed-loop manner, based on optical and chemical assaying feedback. The overall idea is depicted in Figure 1.

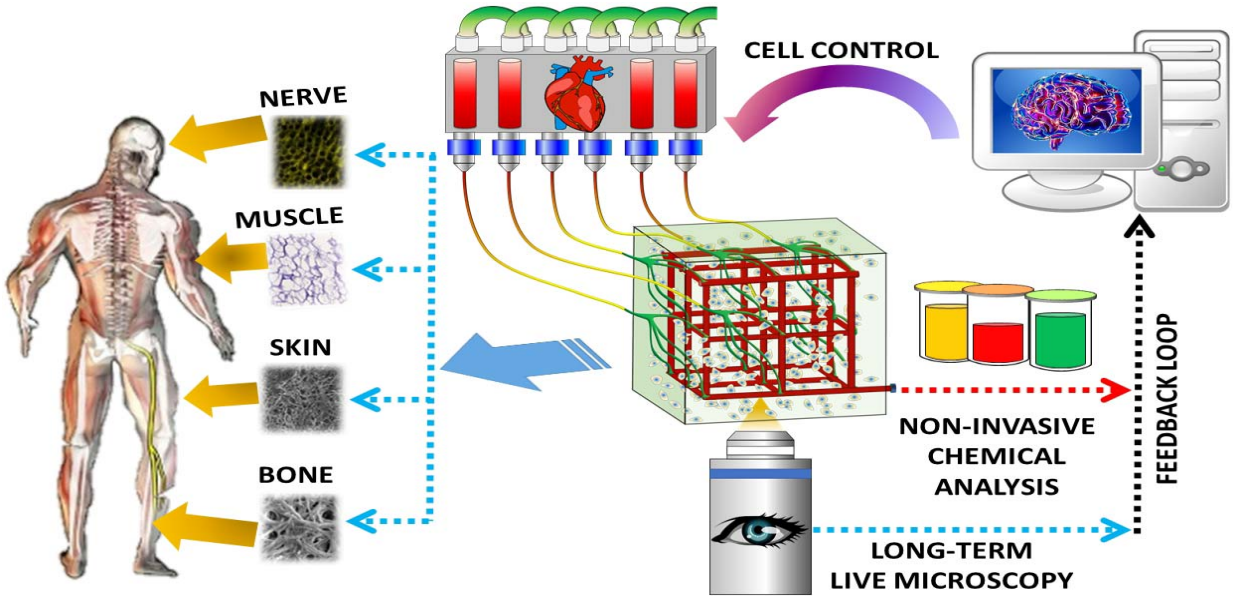

Figure 1 Hypothesized ideal scaffold with *active* "vasculature" that enables targeted real-time fluid and cell manipulation within the cultured tissue. External pumping acts like a "heart", while the whole process is orchestrated by a computer acting like a "brain". The computer's closed-loop responses are based on feedback from non-destructive chemical analysis and long-term live microscopy throughout the entire duration of the culture. Viable artificial tissue is cultured automatically and reproducibly.

We further hypothesize that these goals can be achieved by merging microfluidic and scaffold technologies. Interestingly, microfluidics technologies share many characteristics with conventional biomanufacturing techniques, while at the same time lacking their major bottlenecks (see Table 1). Namely, they have the ability to seed cells with precision, perform nondestructive localized chemical sampling and are transparent to microscopic observation. Moreover, the microfluidic substrates can be fabricated with even more precision than their bioprinted counterparts, but *without the danger of*

damaging cells in the process (since they can be *flowed in post fabrication*). Most importantly, the active "vasculature" of micro-channels allows continuous nutrient delivery / waste removal and enables targeted modulation of cell behavior in a closed-loop manner.

Table 1. Comparison of existing biomanufacturing technologies (rows 2-4) with the proposed microfluidics approach (bottom row). Green = key advantages, Red = fundamental limitations.

Tech Type	Material	Geometry	Seeding	Viability	Vasculature	Analysis	Controls
Artificial Scaffold	Any	Poor to Precise	Random	Excellent	Passive	Bulk	Bulk
De-cellularized Organ	Natural	Natural	Random	Excellent	Passive	Bulk	Bulk
Bio-printing	Very-Limited	Precise	Precise	Poor	Passive	Bulk	Bulk
Microfluidics	Less-Limited	Precise	Precise	Excellent	*Active*	*Localized*	*Localized*

Therefore, the microfluidics scaffolds provide numerous advantages over the conventional tissue engineering approaches. Furthermore, although fabricating microfluidics devices has been a major bottleneck to their adoption by the industry, 3D printers are on the verge of being able to manufacture them.[9, 10] Therefore, it makes sense to integrate scaffolds with the microfluidic technologies, in anticipation of the near future when 3D printing will facilitate their translation to the market.

To that end, several such attempts have been made in the past.[11-18] However, these mostly focused on developing the *materials* and the *fabrication techniques* for manufacturing of the microfluidic scaffolds, while the plumbing necessary for the targeted fluid and cell manipulation within them has not been designed. Specifically, the internal plumbing of such scaffolds should contain dedicated ***ports***, distributed at targeted locations (from here on termed as "addresses"), in order to enable the localized nondestructive manipulation (i.e., delivery/probing) of cells and fluids within the cultures. Yet, this is a significant challenge because the plumbing should be both *scalable* to *large* (organ-sized) scaffold sizes and at the same time be capable of maintaining a *high density* targeting throughout its pore space. The problem is illustrated using a 2D example in Figure 2-LEFT.

In this figure, a *naive* approach is shown, where a 3x3 grid of microfluidic ports is actuated via a separate channel dedicated to each of the addresses. This suffers from: a) Poor scaling – the number of flow channels required to actuate each individual address in the grid scales as X*Y, which is the worst case scenario; and b) Crowding - the spacing available for the channels is limited by the separation distance between the neighboring columns of addresses (which should be as small as possible, in order to ideally be able to manipulate and analyze the culture with a single cell spatial resolution). Fortunately, an old concept in the microfluidics field solves this problem by including orthogonally-blocking channels,[19-21] shown in blue in Figure 2-RIGHT. By using this combination of flow and blocking (i.e., valve actuating) channels, (X+Y) scaling is achieved (i.e., only 3 flow + 3 blocking channels are required, as opposed to a total of 9 dedicated flow channels in the X*Y scaling); and the resolution is no longer limited by the crowding.

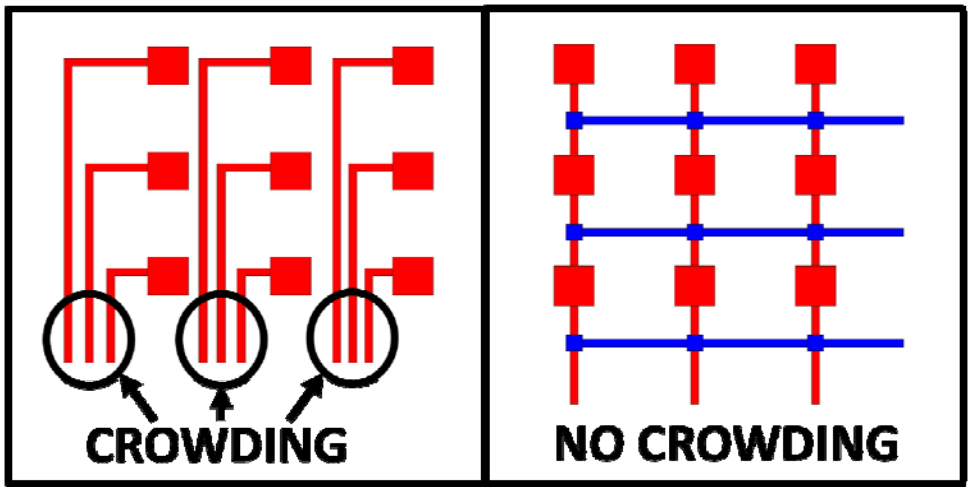

Figure 2 Difference in scalability and resolution of addressable microfluidics arrays, illustrated using a 3 x 3 grid example: LEFT – Inefficient X*Y scaling, and resolution limitations due to crowding of the supply channels; RIGHT – Efficient (X+Y) scaling, and resolution is not limited by crowding. Red = flow channels through which cells or chemicals are delivered and/or sampled; Blue = blocking (i.e., valve actuating) channels.

Thus, the "addressable" microfluidic technologies, such as in Figure 2-RIGHT, yield the *best possible scaling* (e.g., microfluidics chips with over 1000 addresses have been made [22-25]), and the address density is *no longer limited by the crowding*. Therefore, this type of plumbing is the best choice for organ-sized tissue cultures. Yet, it has not been used in microfluidic scaffolds before. Instead, the addresses typically serve as separate *chambers* on chips used for multiple parallel experiments: for example, an array of cell culturing chambers for high-throughput drug testing,[19] a droplet-based device for multi-parameter analysis of single microbes and microbial communities,[20] and a stencil for protein and cell patterning of substrates.[21]

However, here we are interested in addressable fluid manipulation *within a single* cell culture (as opposed to each address corresponding to an isolated chamber), which has not been done before. Furthermore, we want the device to be automated, in order to enable computers to perform the manipulations over long-time culturing experiments. To that end, the remainder of the manuscript presents our proof-of-concept platform, which adapts the addressable microfluidic plumbing and automation, in order to perform the nondestructive cell and chemical manipulations needed to revolutionize tissue engineering scaffolds.

II. MATERIAL AND METHODS

II.1 Materials

Polydimethylsiloxane (PDMS) Sylgard 184 was purchased from Dow Corning (Midland, MI). Negative photoresist SU-8 was purchased from Microchem (Newton, MA). Positive photoresist AZ® P4620 was purchased from Integrated Micro Materials (Texas, USA). Human Fibronectin (Corning®) and

recombinant human platelet-derived growth factor (PDGF-BB) were purchased from VWR (Radnor, PA). Culture media was prepared from Minimum Essential Medium (MEM) (Sigma, MO) supplemented with 10% (v/v) fetal bovine serum (FBS) (VWR, Radnor, PA) and 1% (v/v) penicillin-streptomycin (10,000 U mL-1) (Thermofisher, Waltham, MA). Basal media was composed of MEM supplemented with 1% (v/v) penicillin-streptomycin. For incubation in 5% CO_2 atmosphere, media was buffered by 26 mM sodium bicarbonate (Sigma, MO). CO_2-independent media buffered by 20 mM HEPES (Sigma, MO) was used for microscope stage-top experiments.

II.2 Master Mold Fabrication

The device was fabricated using a multilayer soft-lithography technique.[26] The mold for the device was fabricated using negative photoresist (SU-8) and positive photoresist (AZ® P4620). First, the microscale pattern was sketched using AutoCAD (Autodesk, Mill Valey, CA) and printed at 50,800 dpi on a transparency (Fineline Imaging, Colorado Springs, CO) to generate a high-resolution photomask. Initially, the 4-in silicon wafers (University Wafer, Boston, MA) were washed carefully with diluted soap, rinsed with Acetone, Methanol, DI-water (AMD solvents), dehydrated at 180 ^{o}C for 15 minutes. Subsequently, the wafers were allowed to cool down to room temperature and treated with Hexamethyldisilazane (HMDS) (VWR, Radnor, PA) to enhance the photoresist adhesion. The procedures to create the master mold for each layer of the microfluidic device are describe below:

Control Layer - There were two control layers in the addressable device. The first one was used to actuate the valves in the payload layer (**Figure 5-LEFT**), and the second one was to open/close inlets and outlets of the culture layer (**Figure 3**). The photomasks were switched respectively for each layer and the procedure to create the master mold for the control layer remained the same. Specifically, SU-8 2050 (Microchem, MA) was spin coated at 1500 rpm, exposed to UV light (exposure dose: 240 mJ/cm^2), and developed on a 4-in silicon wafer following the manufacturer's protocol to generate 120-µm height pattern. The developed photoresist was fully crosslinked at 180 ^{o}C for 2 hours, and then slowly cooled down to room temperature.

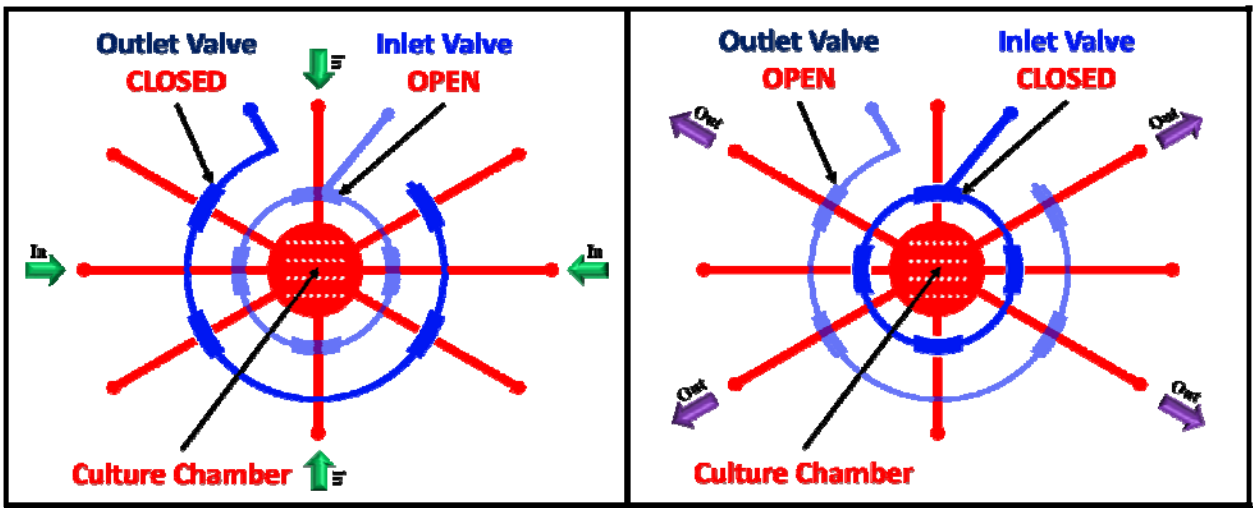

Figure 3 Top XY View of the 'Culture Layer' with the 'Circular Control Valves'. The culture layer is shown in red, and circular control valves are in blue. The fluid can be delivered *into* the culture chamber through the 4 inlet channels (marked with green arrows) when the inlet control valve is "open" and the outlet control valve is "closed" (LEFT), and vice versa (RIGHT); or, the entire culture chamber can be isolated by closing both control valves.

Payload Layer - The master mold for the flow layer consists of two types of photoresists, positive photoresist AZ® P4620 (AZ Electronic Materials, Luxembourg) for the flow channels and negative photoresist SU-8 2150 (Microchem, MA) for the addressable ports. **Round profile flow channels -** AZ® P4620 was spin coated at 1400 rpm, soft-baked at 90 ^{o}C for 10 mins. Then the second layer of AZ® P4620 was spin coated on the same wafer to reach the target coated layer of 28-µm, soft-backed at 90°C for 1 hour. Subsequently, the wafer was rehydrated overnight inside the oven at 37 ^{o}C with an opened water tray (12 hours), exposed to UV light (exposure dose: 2800 mJ/cm^2), and developed to form 28-µm height feature. The round profile of the channels was created by baking the wafer with AZ® P4620 feature at 150 °C on a programmable hot plate for 15 hours, starting at 65 ^{o}C with heating ramp rate of 4 °C/h. **Addressable Ports** - SU-8 2150 was spin coated directly on the same wafer at 1250 rpm, aligned with the first pattern using a custom mask aligner,[27] exposed to the UV (exposure dose: 2800 mJ/cm^2), and developed to generate 550 µm-height square features for the addressable ports. The developed photoresist was fully crosslinked at 180 ^{o}C for 2 hours, cooled down to room temperature, and treated with Perfluorodecyltrichlorosilane (FDTS) (Alfa Aesar, MA) inside the vacuum desiccator chamber for 4 hours.

Culture Layer - The master mold for the culture layer also consisted of two types of photoresists, positive photoresist AZ® P4620 for features, which overlapped with the control valve layer, and negative photoresist SU-8 2150 (Microchem, MA) for the cells culture chamber and non-overlapped flow channels. The round profile features were created by following the same procedure as round profile flow channels for the Payload Layer (see above). Then, SU-8 2035 was spin coated at 1500 rpm, exposed to UV light (exposure dose: 210 mJ/cm^2), and developed on a 4-in silicon wafer by following the manufacturer's protocol to generate 85 µm height square pattern. The developed photoresist was fully crosslinked at 180 ^{o}C for 2 hours and then slowly cooled down to room temperature.

II.3 Microfluidic Device Fabrication

Different PDMS layers of the device were generated using soft lithography. The elastomer with a base-to-agent ratio of 10:1 was poured over the photo-patterned mold to reach the thickness of 5 mm, 1mm, and 2 mm for the payload's control layer, the culture's control layer, and the culture layer, respectively. Then the PDMS casted molds were degassed inside the vacuum desiccator chamber for 2 hours and followed by curing on hotplate at 65 °C overnight (12 hours). The PDMS flexible membranes **(Figure 5.b)** of 35 μm-thickness were created by spin-coating the PDMS with 20:1 base-to-agent ratio onto 4-in silicon wafer at 2500 rpm for 60 seconds then baked at 65°C for at least 1 hour. The cells and/or chemical payload PDMS layer was created by following an established PDMS stencil procedure.[21] Then all the layers were peeled off from the master molds, washed with diluted soap, rinsed with AMD solvents, dried on 180 ^{o}C hotplate, treated with air plasma, and bound to each other using our custom-built UV mask aligner[28] to form the multilayers microfluidic device. The order of binding single layers to form the multilayers microfluidic device was: 1) Cells and/or chemical payload's control layer, 2) 35 μm flexible membrane, 3) Cells and/or chemical payload with addressable ports layer, 4) The control layer for the culture chamber, 5) 35 μm flexible membrane, and 6) Culture layer. A biopsy punch (Electron Microscopy Sciences, PA) with a diameter of 0.5 mm was used to create the inlet and outlet ports for the tubing connection. The whole device was bound on a 50x70 mm glass slide using air plasma.

II.4 Pumping Automation, Experimental Setup, and Microscopy

Here we employ a modification of an open-sourced programmable pneumatic technology, developed for operation and automated control of single- and multi-layer microfluidic devices.[29-31] Following this design, we built a pneumatic system based on modular industrial automation components made by WAGO (see Figure 4**)**. Specifically, the core of the setup was an Ethernet-based programmable WAGO-I/O-SYSTEM 750 logic controller, and an 8-channel digital output module (WAGO Kontakttechnik GmbH & Co, Minden, Germany) that allows the controller to drive 24V Festo (MH1-A-24VDC-N-HC-8V-PR-K01-QM-APBP-CX-DX, Festo, Germany) miniature pneumatic solenoid valves. The solenoid valves were connected to a custom DYI pneumatic pumping system, which deliver the chemoattractant to the addresses. In order to avoid contact between the solenoid valves and the pumped liquid, the system contains machined reservoirs that prevent water from backing up into the solenoid valves. Specifically, the setup operates by sending 24 V digital output to the solenoid valves via an eight-channel digital output module (Wago 750-530). The "on" and "off" positions of the solenoid valves correspond to the "open" and "close" states of the valves on the chip. Switching from "open" to "close" means changing the pressure inside the on-chip valve from atmospheric pressure to 20 psi. The device was connected to media bottles and house-air via Tygon tubing (Cole-Parmer, IL) of 0.02-in inner diameter. The valves in the control layers were automatically operated by miniature pneumatic solenoid valves which were controlled by a programmable WAGO controller. The controller was connected to a computer via an Ethernet

interface. Firstly, a sequence of patterns to be addressed on the device was specified using the custom Matlab GUI (see Figure 4-RIGHT). These patterns were then sent to the WAGO module to toggle the Festo valves, which in turn selectively actuated the on-chip valves at preset locations (specified by the pattern created above) for the delivery of color dye through the ports.

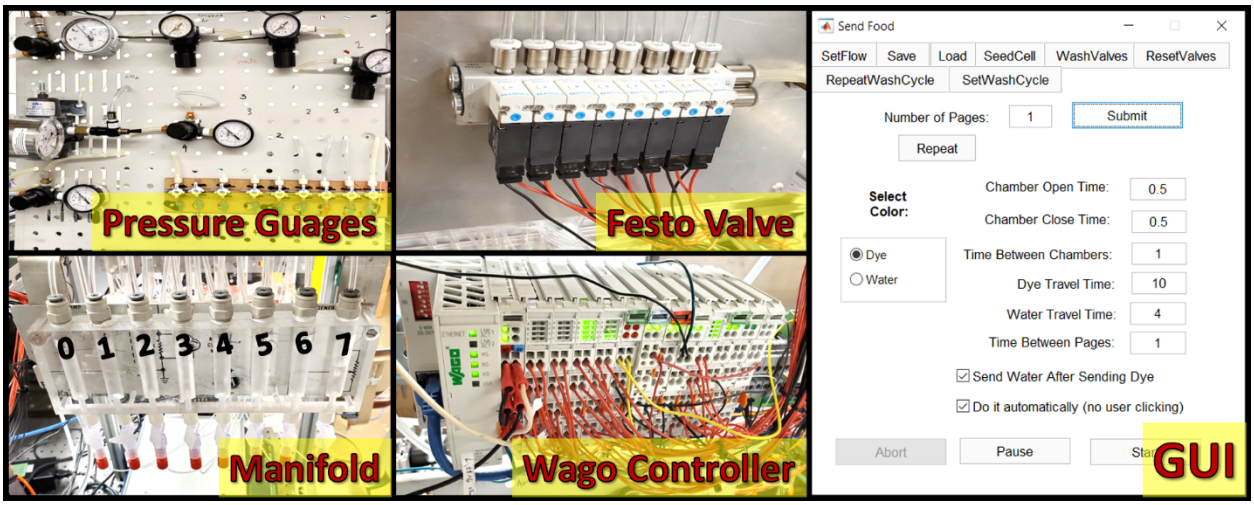

Figure 4 Automated pumping system. LEFT-TOP: pneumatic pumping system; LEFT-BOTTOM: manifold with 8 Festo solenoid valves; CENTER-TOP: water storage machined reservoirs for control channels; CENTER-BOTTOM: Wago controller; RIGHT: custom GUI for controlling the solenoid valves via the Wago controller.

The device was mounted on an automated microscope (IX83, Olympus, Japan) equipped with a XY motorized stage (96S106-O3-LE2, Ludl, NY), and a custom temperature control setup. The images were acquired using a digital CMOS camera (Orca Flash V4, Hamamatsu, Japan). The image acquisition was performed using a custom Matlab (MathWorks Inc., Natick, Massachusetts) GUI.[32]

II.5 Demonstration of Fluid Manipulation within the Device

Since many biochemical agonists are colorless / undetectable by regular microscopes, food dye (Assorted Neon!, McCormick, Baltimore, MD) was used in order to create a visual demonstration of the fluid manipulations within the microfluidic device. The dye was added into media bottles connected to the flow channels of the device via Tygon tubing. Air pressure of ~ 1 psi was used to drive the fluid into the device and across the flow channel. On-chip valves were connected to a pressure source of ~ 20 psi in order to fully obstruct the flow when the valves were in a “closed” state. Matlab code was used to preset the pattern in which the dye was delivered and/sampled. For the latter, the one outlet of the payload channel was connected to the vacuumed vials via Tygon tubing, which played the role of collecting the samples and also dispensing the sampling fluid for analysis by switching between evacuating/pressurizing the vials. Time-lapse video of the dye delivery was recorded using a compact digital microscope (AD4113T, Dino-lite, Torrance, CA).

II.6 Device Preparation for Cell Culturing

The device was autoclaved at 121 ^{o}C for 60 mins to completely cure the uncrosslinked oligomers inside the bulk PDMS, evaporate the remained solvent from curing agent, and sterilize the PDMS device prior to adhesion surface treatment and cell seeding. Subsequently, the cell culture chamber of the device was coated with fibronectin 10ug/mL and the internal surfaces of the microfluidic channels were treated with 2% BSA at 25 ^{o}C (room temperature condition) for at least 10 hours inside the UV chamber to maintain the sterile condition of the PDMS device. In this case, 2% BSA solution was used to prevent the adhesion of the cells to the microfluidic channel's surface.

II.7 Cell Patterning Experiment

Cell Preparation - The chosen cell type was suspended in pre-warmed complete growth DMEM medium supplemented with 10% fetal bovine serum and Gentamicin at the concentration of 50µg/mL to reach the cell concentration of 5 x 10^6 cells mL^{-1}. Initially, cells were trypsinized from a T-75 cell culture flask by adding 2□mL of 1x trypsin/EDTA (0.25%, 0.2□g□L−1 EDTA) for 3□min. DMEM (8□mL) was added to neutralize the trypsin/EDTA activity. The cell suspension was centrifuged at 1000 × g for 2□min. The supernatant was removed by aspiration and the cell pellet was re-suspended in 5ml of Cell-tracker fluorescent dye in PBS (CellTracker™ CM-DiI (Invitrogen™, MA) for red fluorescent cells membrane labeling (λ_{exc} = 553 nm / λ_{em} = 570 nm); CellTracker™ Green CMFDA Dye (Invitrogen™, MA) for green fluorescent cells cytoplasm labeling (λ_{exc} = 492 nm / λ_{em} = 517 nm)). The cells suspension was incubated at 37 ^{o}C for 45 minutes and then centrifuged at 1000 × g for 2□min. The supernatant was removed by aspiration and the cell pellet was re-suspended in DMEM culture media to reach the desired concentration [5 x 10^6 cells mL^{-1}]. Finally, the cell suspension was ready for the cell seeding procedure.

Experiment setup - 10 mL of suspended cells was added to a dispensing bottle with 4 ports that connected to the cell and/or chemical payload channels of the device. The bottle was then pressurized by 5% Carbon dioxide at 6-7 psi under constant shaking motion at 210 rpm. On-chip valves are connected to a pressure source of ~ 20 psi in order to fully close the flow when the valves are in a "close" state. Matlab code was used to preset the patterns, which were used to manipulate the cells and seed them via the addressable ports. The fluorescent and time-lapse images were captured using a fully automated Olympus IX83 microscope fitted with a 20X phase-contrast objective (Olympus, Japan), a CMOS camera (Orca Flash 4.0 V2, Hamamatsu, Japan). Time-lapse images were automatically captured at a 15 minutes interval for duration of 30 hours. For each time step, 121 tile images were acquired at different locations, stitched, and stabilized using an in-house Matlab® 2016b code (MathWorks, Inc., Natick, MA). During acquisition, the culture media was automatically refreshed after 5 hours via the culture layer's flow channels of the device by manipulating the culture's layer control valves "on/off". The composite images

of patterned cell co-cultures created by seeding two different cell types in different locations were assembled using the ImageJ software (National Institutes of Health).[33]

II.8 Data Analysis

The migrating cells were tracked using the Manual Tracking plug-in for ImageJ software.[33, 34] The directional decisions chosen by each individual cell at the bifurcation were determined via manual observation. Quantitative data of cell sequences was generated using an in-house Matlab® 2016b code (MathWorks, Inc., Natick, MA). Significance level was determined by using a non-parametric test for a binomial distribution, unless otherwise stated. Statistical significance was set as $p < 0.05$.

III. RESULTS

III.1 Redesigned Microfluidic Plumbing for Addressable Access to the Culturing Layer

In this manuscript, we have realized an envisioned proof-of-concept automated microfluidic platform, capable of nondestructive XY fluid manipulation within live 2D cultures. To do this, we used a combination of micro-sized flow channels and blocking pneumatic valves, in order to actuate the individual addresses *independently* of each other. After going through multiple iterations of the plumbing design, we have converged upon the result shown in Figure 5-LEFT. There, the addressable array has a 4x4 size for simplicity, though the actual grid size is a free parameter. Each of the addresses in the array are shown as red-discs and are surrounded by O-shaped pneumatic valves (shown as blue circles). When the valve is "*closed*" (see the inset in Figure 5-LEFT), the fluid traveling through the red channels is re-routed around the address via a thin bypass channel (also labeled in red). However, when a valve is "*open*", the corresponding address can either deliver or withdraw (depending on the direction of the flow in the red channels) the fluid carrying a chemical payload, and/or cells, to/from the culture layer below (see Figure 5-RIGHT).

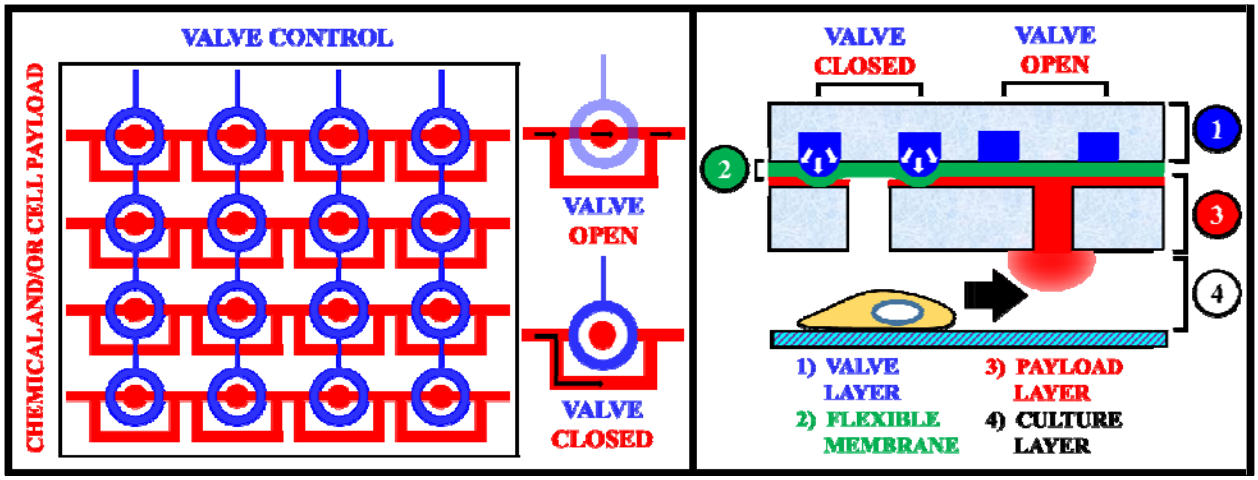

Figure 5 Schematic of the Addressable Microfluidic Plumbing. (LEFT) Top XY view of a 4x4 matrix of "addressable" ports. Flow channels are shown in red, and blocking valve channels are in blue. Inset shows that a

port is active when the valve is "open", and bypassed when it is "closed". Black arrows indicate direction of flow, which assumes payload *delivery* to (as opposed to *sampling* at) an address. (RIGHT) Z cross-section of the same device, showing how a cell neighboring an open microfluidic port is attracted towards chemical payload released through it into the 'culture layer'. At the same time, it is shown that the closed port directly above it, does not affect the cell.

Figure 5b is a Z cross-section of the device, which shows that it consists of 4 main layers (from top to bottom): a valve layer, a thin flexible membrane, a flow layer, and a cell culture layer. The action of the O-shaped valve is also shown in the same figure: in the *"closed"* state, the pressurized valve expands, causing the flexible membrane to block flow to the address; conversely, in the "*open*" state, the flow is allowed to enter the address freely, where a microfluidic port then connects it with the culture layer below. As an example, a chemical payload can be delivered through this port in order to attract a neighboring cell. At the same time, the *closed* port directly above the cell would not affect its behavior.

III.2 Nondestructive *Fluid* Manipulation within the Culture Layer

Some possible fluid and/or cell manipulations within the device are: 1) Seeding different cell types in varied amounts and pre-determined patterns; 2) Nourishing them by continuously renewing the culture media, or inducing directed migration by establishing a nutrient or a chemoattractant gradient; 3) Patterning tissue by modifying cell behavior and/or morphology via delivery of bio-agonists (e.g. growth, differentiation factors) and/or drugs(e.g., cytoskeleton-altering) to specified locations/selected cells within the device; and 4) Sampling a living culture non-invasively, by picking up and, sending off for analysis, effluents from different locations above the cells.

The action of delivering and sampling chemicals within the addressable device is shown in the left and right panes of Figure 6, respectively. In the former case, a purple dye is delivered to the right bottom corner of a 4x4 array of microfluidic ports; while in the latter case, the same purple dye is withdrawn back via a port at the opposite end of the same address row. As a possible application, the picked up fluid could be a cell culture effluent, which would then be sent off to an ex-situ sensor for non-destructive analysis. This would eliminate the reliance on destructive chemical assays, ensuring continuous monitoring of the biology occurring within live cultures. Furthermore, it can be done continuously over long period of time, given that the whole process is automated, and as such, does not require any human involvement. Video 1 shows the operation of the device over time.

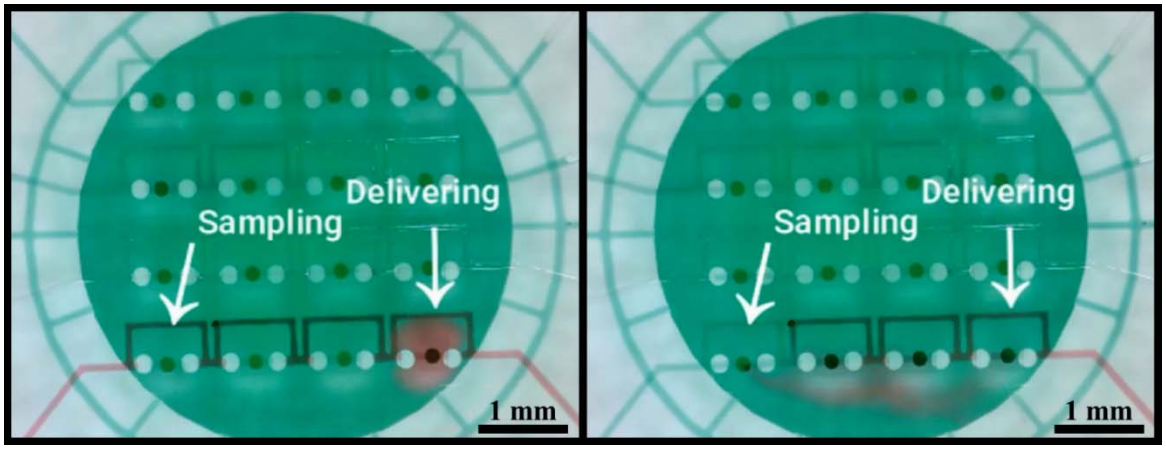

Figure 6 Microscopy of the fluid manipulation within the culture layer. LEFT - delivery of a purple dye to the bottom right corner port in the 4x4 grid; RIGHT - sampling of the delivered purple dye via the bottom left corner port in the 4x4 grid. . Each port is 150 µm in diameter, and the channels are 100 µm in width.

III.3 Nondestructive *Cell* Manipulation within the Culture Layer

To further demonstrate the addressable device's ability to manipulate *cells* within the Culture Layer, its ports were used for seeding (i.e., additive manufacturing) a co-culture of mouse Mesenchymal Stem Cell (MSC) and Fibroblasts (NIH3T3) in a predetermined pattern. Video 2 shows the process of the cell delivery through a single port to the Culture Layer below, and Figure 7-LEFT shows the MSCs (green) seeded in a square shape that surrounds the NIH3T3s (red) deposited in its center.

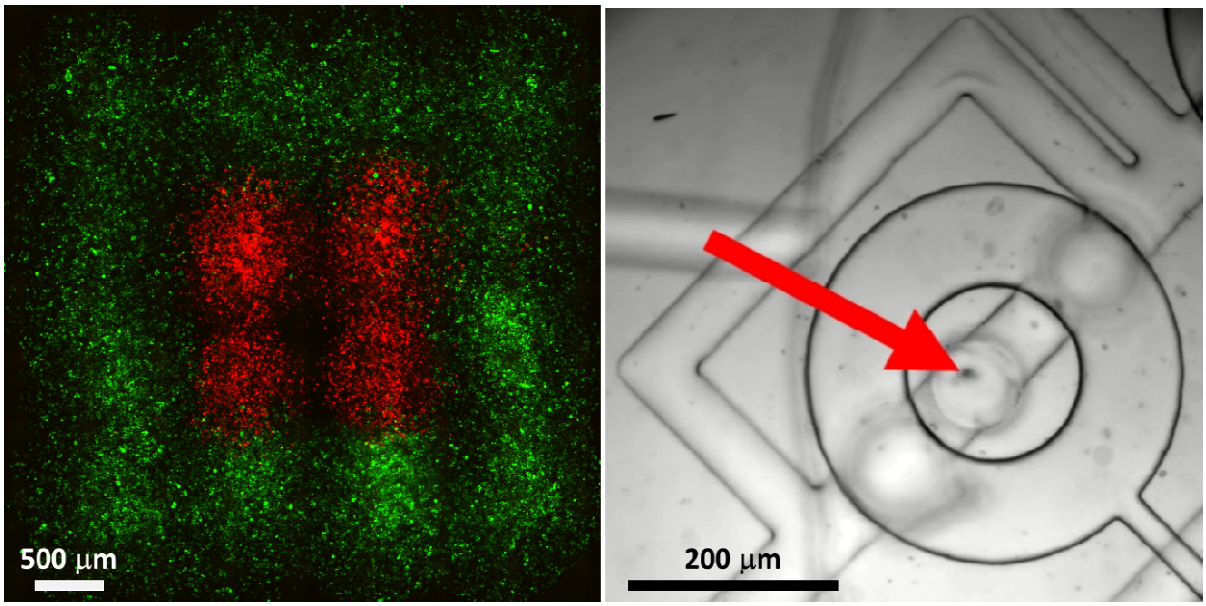

Figure 7 Nondestructive *additive* cell manipulations within the Culture Layer of the device. LEFT- Fluorescence panorama showing MSCs (green) seeded in a square pattern, with NIH-3T3s (red) in its center. Pane size is ~4.5mm x 4.5mm. RIGHT - Phase microscopy image showing the ability to trap and manipulate a single cell at a time (red arrow).

Furthermore, Figure 7-RIGHT and Video 3 show the device's ability to trap single cells by the O-valve. This means that the additive manufacturing can be done with single cell precision, for example in order to create seeding density gradients. Finally, Figure 8 shows a density gradient created by delivering progressively increasing amounts of the MSCs to a row of addresses from left to right.

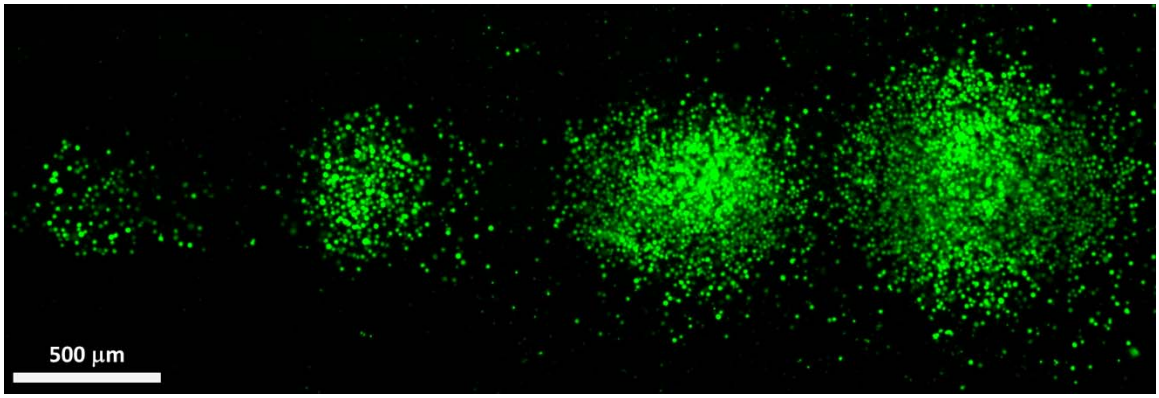

Figure 8 Fluorescent microscopy of nondestructive *additive* cell manipulations within the Culture Layer of the device: a MSC seeding density gradient, increasing from left to right. Panorama is ~1.3mm x 4mm.

The next step is to demonstrate *inverse* patterns via *subtractive* manufacturing. The idea is to cleave focal adhesions that are anchoring confluent cells to the bottom of the substrate, by delivering Trypsin in pre-determined patterns. The lifted cells will then be drawn in via pressure reversal through the microfluidic ports and sent for *ex-situ* analysis.

IV. DISCUSSION

The goal of this work was to create a technology capable of real time nondestructive manipulation of cells and fluids within living cultures of artificial tissues. A major disadvantage of the existing biomanufacturing methods is the disconnect that currently exists between the scaffold fabrication and its culturing: namely, once the cells are either seeded or bioprinted into conventional scaffolds, all access to them is lost for the remainder of the culturing duration. As a result, the existing controls over cell behavior are typically done in one of the following ways: A) Scaffolds – substrate shape, stiffness, charge, porosity and chemical composition are typically used to affect cell behavior; B) Biologicals – various growth and differentiation factors, antiseptics and other drugs / biomolecules are either added to the cell culture media, or released from the scaffold over time; the cells' DNA is modified to express or knockout a certain feature of interest; foreign microorganisms are introduced to produce synergic interactions and signaling queues; and C) Physicomechanical – shaking, mechanical loads etc. are applied to enhance the culture.[35]

However, the overarching limitation of these *fabrication-based* controls is that they are either *static*, in the sense that they do not vary over time (e.g. substrate material, shape); or, are "blind" (aka,

open-loop), as in the case of the timed-drug release from scaffolds. In other words, the stimuli do not adapt in response to the cell behavior. Furthermore, after the cells are either seeded or bioprinted into the scaffold, they cannot be targeted precisely. Consequently, only *bulk level* monitoring (e.g., probing the temperature and the pH of the bioreactor effluent) and controls (e.g., adjusting the media contents and the bioreactor environment) are available during the culturing stage of the artificial tissue manufacturing. So the culture-based controls are not only poor in a sense that there is little feedback available, but they have negligible spatial resolution as well. Yet, precise closed-loop controls over *localized* cell behavior throughout the *entire* culturing process are necessary for producing viable tissue and maintaining product consistency. For example, in vivo organogenesis occurs in *multiple-steps*; this is illustrated by how most bones in our bodies start out as cartilage, and only subsequently become calcified through a process called endochondral ossification. Thus, in order to replicate such dynamic processes in vitro, both *spatial* and *temporal* control over the tissue development is required.

For this reason, several attempts have been made in the past to create the microfluidic scaffolds;[11-18] most notably, Bob Langer's,[12] who is regarded as one of the founders of tissue engineering. The idea is that the integration of "vasculature" into the scaffolds can potentially resolve product size limitations and yield consistent tissue quality. Specifically, a combination of micro channels and ports could be utilized for patterning tissue by flowing different types of cells into the desired positions; overcoming product-size limitations[36] by nourishing the cells deep within *large* scaffolds, ; enabling long-term survival of the cells in artificial environments by clearing metabolic waste from the scaffold pore space; and controlling the tissue growth in an adaptive manner by modulating the cell behavior, based on nondestructive microscopy and ex-situ chemical assay analysis (which could also be accomplished by using the microfluidic ports to sample the culture effluent). These abilities would result in improved cell viability compared to conventional biomanufacturing methods (e.g., in bioprinting many cells die as a result of the need to participate in the fabrication process), and in much needed spatiotemporal control over the cell behavior within the living cultures. This would in turn clear major bottlenecks to the advancement of organ manufacturing and drug testing using organ mimics. However, mostly only materials for these scaffolds were developed in the past, while the microfluidic plumbing necessary for the targeted fluid and cell manipulations at different locations within the scaffolds has not been developed.

To that end, we hypothesized that an *addressable* microfluidic plumbing design could be modified in order to enable the nondestructive cell and/or chemical delivery and/or removal/sampling, at targeted locations within the artificial tissue scaffolds. As proof of concept, we fabricated a prototype device, which is capable of performing the said operations within a 2D cell culture. Furthermore, we automated the device, in order to eliminate the reliance on human labor over the long term culturing

periods that are typically expected in tissue engineering experiments. Consequently, we have shown that the device is capable of a localized payload (both fluid and cell) delivery and sampling, directly below any activated address. Furthermore, we have used this technology to demonstrate both additive and subtractive manufacturing, by creating various co-culture seeding patterns and using trypsin release to detach the cells at selected locations.

In principle, single cell behavior such as migration, differentiation, proliferation and tissue deposition could all be controlled using this approach, throughout the entire culturing process (currently not possible using existing biomanufacturing methods). Moreover, this complementary "marriage" of the two technologies would blur the line between fabrication and culturing stages of the tissue-manufacturing process. Instead, it would make the entire process *continuous*, thereby allowing to retain the precision, and the control over individual cells in the scaffold, well into the culturing stage. However, there are still technological difficulties that need to be overcome in order to advance the 2D prototype to a fully-fledged 3D scaffold: namely, 1) The addressable microfluidics plumbing needs to be scaled up for XYZ delivery / sampling (instead of just XY); 2) To facilitate mass production of the 3D scaffolds, a manufacturing method that is free of manual layer-by-layer alignment needs to be developed. There are several potential candidate technologies that could be used for this in the near future. Namely, digital micro-mirror device projection printing (DMD-PP) is a stereolithographic method that uses an array of micro-mirrors to spatially modulate a pulsed UV laser, in order to achieve additive crosslinking patterns in a photo-curable material.[16, 37-40] Similarly, it can also be used for subtractive laser ablation within previously crosslinked layers of the material. An alternative approach is to 3D print a *sacrificial* mold (a.k.a. "template"), shaped like the inverse of the desired scaffold pore network.[15] The template is then submerged into a gel precursor of the scaffold material. After the gel has solidified around the template, the latter is dissolved out of the gel, leaving behind the desired porous networks in the scaffold. 3) Finally, the scaffold should be biocompatible and *biodegradable* when implanted in vivo. As mentioned before, there are a number of candidate materials that have been custom-designed specifically for fabricating the microfluidic scaffolds: such as poly(ester amide), poly(1,3-diamino-2-hydroxypropane-co-polyol sebacate) (APS)[14], poly(glycerol-co-sebacate) (PGS),[13] poly(octamethylene maleate (anhydride) citrate) (POMaC),[17] Poly(ethylene glycol) diacrylate (PEGDA),[15] poly(l-lactic-co-glycolic) (PLGA)[11], and Silk fibroin[13, 18]. However, given that the scaffolds in these studies did not utilize the use of microfluidic valves, it is not apparent whether these materials are stiff enough to make them. Only the silk fibroin has been used to create such valves, but it is not a crosslinkable material,[18] so it is currently not compatible with the 3D stereolithographic fabrication methods such as the DMD-PP. Therefore, further work should be done in order to develop new cross-linkable,

biodegradable/biocompatible, materials that are stiff enough to create microfluidic valves, and that would ideally be optically transparent for microscopy observation.

Overall, the successful development of microfluidic scaffolds will help to minimize the crippling tissue variability plaguing the biomanufacturing industry today. This will benefit patients in need of life-saving transplants by accelerating the translation of regenerative medicine technologies to the clinical market. Moreover, the nondestructive visual and chemical observation of the cell behavior in the 3D artificial tissue cultures will lower experiment costs and provide data-gathering continuity superior to the conventional analysis (i.e., destructive chemical assays for each time point). Ultimately, the proposed approach will pave the way toward tracking and controlling of every cell in a culture on an individual basis, given that its targeting precision is limited only by the fabrication quality of the scaffold (to be refined tremendously by the anticipated explosion of 3D printed microfluidics[6, 7]). This will shift the tissue engineering paradigm from integrating "blind" (i.e., open-loop) controls into the scaffold's material (e.g., timed drug release) to controlling cells in growing tissues interactively instead. Finally, the computer-driven culturing would solve a major logistical hurdle to the adoption of such technologies by allowing companies to provide digital codes to hospital staff, instead of having to teach them custom culturing protocols for each new product (which is impractical). This would both simplify the process for the end-user and ensure specification-compliance on-site.

V. CONCLUSION

We have presented a microfluidic platform capable of performing spatiotemporal manipulations of chemicals and cells within a living culture. Specifically, we have interlaced a PDMS prototype with addressable microfluidic ports, and demonstrated that it is capable of both delivering and sampling fluids to the cell culture layer situated at the bottom of the chip. Furthermore, we have shown additive manufacturing by creating spatial seeding patterns by flowing fluorescent MSCs and NIH3T3s into different locations within the device. Lastly, we also demonstrated subtractive manufacturing by detaching selected cells via localized trypsin delivery, and removing them from the culture by drawing them out through the addressable ports. In the near future, we will extend this concept to XYZ manipulations within transparent, biocompatible and biodegradable 3D scaffolds. It is our hope that the design will ultimately resolve the bottlenecks plaguing tissue engineering technologies today, and ultimately enable computer-driven tissue engineering through coupling with automation electronics. Specifically, the proposed technology would enable: 1) organ-sized engineered tissue via nutrient delivery and metabolic waste removal throughout the scaffold; 2) viable and consistent tissue products via orchestration of cell action during culturing; 3) improved drug screening via nondestructive sampling of cell responses throughout the entire time course of administration; 4) biomanufacturing automation for

achieving desired specifications on site, without the need to train hospital staff custom culturing protocols for every different tissue engineering product. This would, in turn, allow machines to culture tissue reproducibly, and without the need to train hospital staff onsite.

VI. ACKNOWLEDGEMENTS

The authors would like to thank Gustavus and Louise Pfeiffer Research Foundation Major Investment Grant, New Jersey Health Foundation Research Award - Grant #PC 22-19, NJIT Faculty Seed Grant, and NSF I-Corps Site - Grant #1450182 for their gracious funding of our work. Additionally, the authors would like to thank New Jersey Institute of Technology (NJIT)'s McNair Achievement and Provost Summer Research Programs for providing student labor for this project. Finally, we would like to thank Dr. Rafael Gómez-Sjöberg for providing us with software and blueprints for the addressable microfluidic technology published on his website.

VII. COMPLIANCE WITH ETHICAL STANDARDS

Funding: This work was supported by the Gustavus and Louise Pfeiffer Research Foundation's Major Investment Grant, New Jersey Health Foundation Research Award - Grant #PC 22-19, NJIT Faculty Seed Grant, and NSF I-Corps Site - Grant #1450182.

Competing Interests: The authors declare that a Provisional U.S. patent Application No. 62/753,622 filed on Oct 31, 2018.

Ethical approval: This article does not contain any studies with human participants or animals performed by any of the authors.

VIII. REFERENCES

1. Administration, U.S.F.a.D. *Approved Cellular and Gene Therapy Products*. [cited 2018 02/20/2018]; Available from: https://www.fda.gov/BiologicsBloodVaccines/CellularGeneTherapyProducts/ApprovedProducts/default.htm.

2. Administration, U.S.F.a.D. *Approved Cellular and Gene Therapy Products*. 2019 [cited 2019 06/17/2019]; Available from: https://www.fda.gov/vaccines-blood-biologics/cellular-gene-therapy-products/approved-cellular-and-gene-therapy-products.
3. Langer, R. and J.P. Vacanti, *Tissue Engineering*. Science, 1993. **260**(5110): p. 920-926.

4. Park, J.Y., et al., *3D printing technology to control BMP-2 and VEGF delivery spatially and temporally to promote large-volume bone regeneration.* Journal of Materials Chemistry B, 2015. **3**(27): p. 5415-5425.
5. Lee, J.-S., et al., *Three-dimensional cell printing of large-volume tissues: Application to ear regeneration.* Tissue Engineering Part C: Methods, 2017. **23**(3): p. 136-145.
6. Wu, P.-H., et al., *Three-dimensional cell migration does not follow a random walk.* Proceedings of the National Academy of Sciences, 2014. **111**(11): p. 3949-3954.
7. Dlouhy, B.J., et al., *Autograft-derived spinal cord mass following olfactory mucosal cell transplantation in a spinal cord injury patient: Case report.* Journal of Neurosurgery: Spine, 2014. **21**(4): p. 618-622.
8. Hunsberger, J., et al., *Manufacturing road map for tissue engineering and regenerative medicine technologies.* Stem Cells Translational Medicine, 2015. **4**(2): p. 130-135.
9. Naderi, A., N. Bhattacharjee, and A. Folch, *Digital Manufacturing for Microfluidics.* Annual review of biomedical engineering, 2019. **21**: p. 325-364.
10. Bhattacharjee, N., et al., *The upcoming 3D-printing revolution in microfluidics.* Lab on a Chip, 2016. **16**(10): p. 1720-1742.
11. King, K.R., et al., *Biodegradable microfluidics.* Advanced Materials, 2004. **16**(22): p. 2007-2012.
12. Bettinger, C.J., et al., *Three-dimensional microfluidic tissue-engineering scaffolds using a flexible biodegradable polymer.* Advanced materials, 2006. **18**(2): p. 165-169.
13. Bettinger, C.J., et al., *Silk fibroin microfluidic devices.* Advanced Materials, 2007. **19**(19): p. 2847-2850.
14. Wang, J., et al., *Biodegradable microfluidic scaffolds for tissue engineering from amino alcohol-based poly (ester amide) elastomers.* Organogenesis, 2010. **6**(4): p. 212-216.
15. Miller, J.S., et al., *Rapid casting of patterned vascular networks for perfusable engineered 3D tissues.* Nature materials, 2012. **11**(9): p. 768.
16. Cha, C., et al., *Structural reinforcement of cell-laden hydrogels with microfabricated three dimensional scaffolds.* Biomaterials science, 2014. **2**(5): p. 703-709.
17. Zhang, B., et al. *Microfluidic tissue: A biodegradable scaffold with built-in vasculature for cardiac tissue vascularization and surgical vascular anastomosis*. in *Proceedings of the Seventeenth International Conference on Miniaturized Systems for Chemistry and Life Sciences*. 2013.
18. Zhao, S., et al., *Bio-functionalized silk hydrogel microfluidic systems.* Biomaterials, 2016. **93**: p. 60-70.
19. Wang, H.-Y., N. Bao, and C. Lu, *A microfluidic cell array with individually addressable culture chambers.* Biosensors and Bioelectronics, 2008. **24**(4): p. 613-617.
20. Leung, K., et al., *A programmable droplet-based microfluidic device applied to multiparameter analysis of single microbes and microbial communities.* Proceedings of the National Academy of Sciences, 2012. **109**(20): p. 7665-7670.
21. Gao, Y., et al., *Digital microfluidic programmable stencil (DMPS) for protein and cell patterning.* RSC Advances, 2016. **6**(104): p. 101760-101769.
22. Thorsen, T., S.J. Maerkl, and S.R. Quake, *Microfluidic large-scale integration.* Science, 2002. **298**(5593): p. 580-584.
23. Melin, J. and S.R. Quake, *Microfluidic large-scale integration: the evolution of design rules for biological automation.* Annu. Rev. Biophys. Biomol. Struct., 2007. **36**: p. 213-231.
24. Mark, D., et al., *Microfluidic lab-on-a-chip platforms: requirements, characteristics and applications.* Chemical Society Reviews, 2010. **39**(3): p. 1153-1182.
25. Araci, I.E. and P. Brisk, *Recent developments in microfluidic large scale integration.* Current opinion in biotechnology, 2014. **25**: p. 60-68.

26. Unger, M.A., et al., *Monolithic microfabricated valves and pumps by multilayer soft lithography.* Science, 2000. **288**(5463): p. 113-6.
27. Pham, Q.L., et al., *A compact low-cost low-maintenance open architecture mask aligner for fabrication of multilayer microfluidics devices.* Biomicrofluidics, 2018. **12**(4): p. 044119.
28. Li, X., et al., *Desktop aligner for fabrication of multilayer microfluidic devices.* Review of Scientific Instruments, 2015. **86**(7): p. 075008.
29. Gómez-Sjöberg, R., et al., *Versatile, fully automated, microfluidic cell culture system.* Analytical chemistry, 2007. **79**(22): p. 8557-8563.
30. Brower, K., et al., *An open-source, programmable pneumatic setup for operation and automated control of single-and multi-layer microfluidic devices.* HardwareX, 2018. **3**: p. 117-134.
31. **Gómez-Sjöberg, R.** *Rafael's Microfluidics Page*. Available from: https://sites.google.com/site/rafaelsmicrofluidicspage/home.
32. Pham, Q.L., et al., *Open-Source Matlab-Based Graphical User Interface (GUI) For Computer Control of Microscopes Using Micro-Manager.* arXiv preprint arXiv:1904.13231, 2019.
33. Schneider, C.A., W.S. Rasband, and K.W. Eliceiri, *NIH Image to ImageJ: 25 years of image analysis.* Nat Methods, 2012. **9**(7): p. 671-5.
34. Cordeli, F., *Manual Tracking Plug-in for ImageJ.* 2005: Institut Curie , Orsay (France).
35. Fernandez-Yague, M.A., et al., *Biomimetic approaches in bone tissue engineering: Integrating biological and physicomechanical strategies.* Advanced drug delivery reviews, 2015. **84**: p. 1-29.
36. Novosel, E.C., C. Kleinhans, and P.J. Kluger, *Vascularization is the key challenge in tissue engineering.* Advanced drug delivery reviews, 2011. **63**(4): p. 300-311.
37. Warner, J., et al., *Design and 3D Printing of Hydrogel Scaffolds with Fractal Geometries.* Acs Biomaterials Science & Engineering, 2016. **2**(10): p. 1763-1770.
38. Zhang, A.P., et al., *Rapid Fabrication of Complex 3D Extracellular Microenvironments by Dynamic Optical Projection Stereolithography.* Advanced Materials, 2012. **24**(31): p. 4266-+.
39. Hribar, K.C., et al., *Light-assisted direct-write of 3D functional biomaterials.* Lab on a chip, 2014. **14**(2): p. 268-275.
40. Yang, W., et al., *Rapid fabrication of hydrogel microstructures using UV-induced projection printing.* Micromachines, 2015. **6**(12): p. 1903-1913.